by taking into account the motion of the surrounding chains. The experimental data give $J_e^\circ \propto \phi^{-2}$ for the concentration dependence of the limiting compliance: that means that the average spacing between entanglements N_e varies as ϕ^{-1}, in agreement with the reptation model with or without tube renewal effects. Our model explains reasonably the variations of the terminal relaxation time, its value being clearly influenced by tube renewal when the entanglement density is weak, i.e., $\phi M/M_e$ lower than about 30–50. In the same range of concentrations, our model predicts correctly the empirical law for zero-shear viscosity: $\eta_0/\zeta_0 \propto \phi^{3.4-3.5}$. But for strongly entangled solutions ($\phi M/M_e > 60$–50), the reptation is dominant and data of the literature show that, in this case $\tau_0/\zeta_0 \propto \phi^1$ and $\eta_0/\zeta_0 \propto \phi^3$. Within the same range, the molecular weight dependence remains $\eta_0/\zeta_0 \propto M^{3.4-3.6}$, confirming that tube renewal is not an explanation for the discrepancy between experiment and theory as far as the molecular weight dependence is concerned.

References and Notes

(1) Ferry, J. D. "Viscoelastic Properties of Polymers"; Wiley: New York, 1980; Chapter 17, p 486.
(2) Isono, Y.; Fujimoto, T.; Takeno, N.; Kjiura, H.; Nagasawa, M. *Macromolecules* **1978**, *5*, 888.
(3) Berry, C. G.; Nakayasu, H.; Fox, T. G. *J. Polym. Sci., Polym. Phys. Ed.* **1979**, *17*, 1825.
(4) Orbon, S. J.; Plazek, D. J. *J. Polym. Sci., Polym. Phys. Ed.* **1979**, *17*, 1871.
(5) Marin, G.; Menezes, E. V.; Raju, V. R.; Graessley, W. W. *Rheol. Acta* **1980**, *19*, 462.
(6) Raju, V. R.; Menezes, E. V.; Marin, G.; Graessley, W. W. *Macromolecules* **1981**, *14*, 1668.
(7) Berry, C. G.; Fox, T. G. *Adv. Polym. Sci.* **1968**, *5*, 261.
(8) Graessley, W. W. *J. Chem. Phys.* **1971**, *54*, 5143.
(9) Doi, M.; Edwards, S. F. *J. Chem. Soc., Faraday Trans. 2* **1978**, *74*, 1818.
(10) Graessley, W. W. *Adv. Polym. Sci.* **1974**, *16*, 1.
(11) Montfort, J. P.; Marin, G.; Monge, Ph. *Macromolecules* **1984**, *17*, 1551.
(12) Klein, J. *Macromolecules* **1978**, *11*, 852; *Polym. Prepr., Am. Chem. Soc., Div. Polym. Chem.* **1981**, *22*, 105.
(13) Graessley, W. W. *Adv. Polym. Sci.* **1982**, *47*, 67.
(14) Fox, T. G.; Flory, P. J. *J. Appl. Phys.* **1950**, *21*, 581.
(15) Ninomiya, K.; Ferry, J. D.; Oyanagi, Y. *J. Phys. Chem.* **1963**, *67*, 2297.
(16) Plazek, D. J.; O'Rourke, V. M. *J. Polym. Sci., Part A* **1971**, *9*, 209.
(17) Gray, R. W.; Harrison, G.; Lamb, J. *Proc. R. Soc. London, Ser. A* **1977**, *356*, 77.
(18) Flory, P. J. *J. Chem. Phys.* **1949**, *17*, 303.
(19) Raju, V. R.; Rachapudy, H.; Graessley, W. W. *J. Polym. Sci., Polym. Phys. Ed.* **1979**, *17*, 1223.
(20) Graessley, W. W.; Raju, V. R. *J. Polym. Sci., Polym. Symp.* **1984**, *No. 71*, 77.

Chain Statistics of Poly(diacetylenes) in Solution

G. Allegra and S. Brückner*

Dipartimento di Chimica del Politecnico, 20133 Milano, Italy

M. Schmidt and G. Wegner

Max-Planck Institut für Polymerforschung, D-6500 Mainz, West Germany.

Received May 21, 1985

ABSTRACT: Light-scattering results from dissolved poly(diacetylene) chains (Wenz, G.; Müller, M. A.; Schmidt, M.; Wegner, G. *Macromolecules* **1984**, *17*, 837) may be quite satisfactorily interpreted on the basis of a single rotational isomer undergoing twisting and bending fluctuations, their amplitude being directly derived from IR force constants. The usual rotation-matrix algorithm is adopted. Randomly introducing a $^1/_6$ fraction of ±90° rotations around the triple bonds of the structure $-(CR{=}CR{-}C{\equiv}C-)_N$ to account for the specifically observed conjugation length, the mean-square chain size shrinks by less than 7% (the persistence length decreases from 190 to 177 Å); inaccuracy in the force constant adopted for twisting around the C=C bond and perhaps excluded-volume effects may account for the difference. It is shown that both models are very well represented by an ideal wormlike chain with the proper persistence length. No significant amount of either the cis conformation of the double bonds or the cumulene structure $=(CR{-}CR{=}C{=}C{=})_N$ is compatible with observation, in that they would cause a drastic reduction of the chain size.

Introduction

As first shown by Wegner in 1960,[1] poly(diacetylenes) (PDA) may be synthesized as macroscopic single crystals by solid-state polymerization.[2-7] X-ray analysis indicates that the structure is close to a regular sequence of double and triple bonds separated by single bonds, as shown in Figure 1a.[8,9] Although additional evidence from spectroscopic investigations confirms this structure to be the most important, it suggests that the resonance structure reported in Figure 1b may also play some role, thus stabilizing chain planarity.[10] More recently, it has been shown[11] (henceforth quoted as paper 1) that suitably substituted PDA's may be dissolved in appropriate solvents, thus opening the way to a vast field of physicochemical studies. In particular, in paper 1 extensive investigations were reported on PTS-12 and P3BCMU (see Table I) dissolved in $CHCl_3$, CH_2Cl_2, and dimethylformamide. Amid a series of interesting results, it was shown that both polymers (i) display features analogous to those of the wormlike (Porod–Kratky) chain model, the persistence length l_{pers} being in the range 150–200 Å for PTS-12, and (ii) may be described as consisting of seg-

Table I
Two Examples of Soluble Poly(diacetylenes) of General Structure

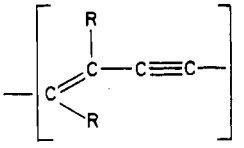

	R
PTS-12	$(CH_2)_4OSO_2C_6H_4CH_3$
P3BCMU	$(CH_2)_3OCONHCH_2CO_2$-*n*-C_4H_9

0024-9297/86/2219-0399$01.50/0

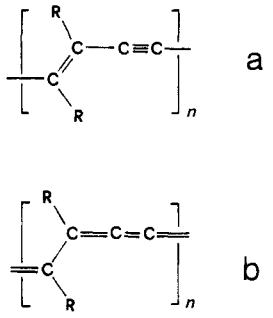

Figure 1. Two possible resonance forms of PDA.

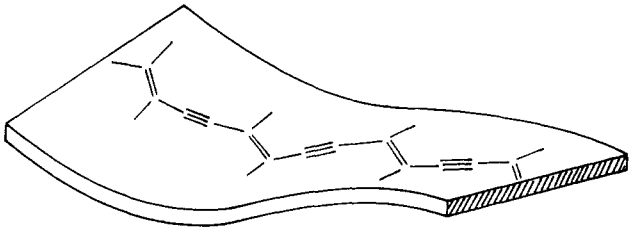

Figure 2. Fully conjugated PDA chain may behave like a ribbon slowly twisting and bending ("ribbon wormlike chain", also denoted as model 1 in the text).

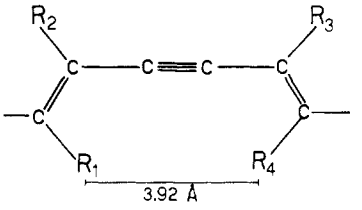

Figure 3. Scheme showing a cisoid conformation across the C—C≡C—C sequence. The indicated distance refers to the first C atoms of the side groups that are bonded to the chain (C_R); the same parameters as in Figure 4 are used, with (C=C—C_R) = 120° and d(C—C_R) = 1.50 Å.

ments of effective conjugation length approximately spanning 5–7 monomeric units, in contrast with the crystal-state results where this length is substantially larger.

The paucity of theoretical results pertaining to dissolved polymer chains where the skeletal rotations are hindered by conjugation effects prompted us to undertake the present conformational and statistical investigation. Our analysis, aimed at proposing an interpretation for the above reported facts, is based on models wherein most of the molecular flexibility derives from small, elastic deformations of bond angles and rotation angles.

Two Conformational Models

According to current views, full π-conjugation extending throughout the chain would only be compatible with an essentially planar chain conformation, which continuously bends and twists as shown in Figure 2. Actually, in addition to the transoid conformation across the C—C≡C—C sequence, as represented in the figure, the cisoid arrangement might also preserve π-conjugation. In the latter case side groups belonging to neighboring units (R_1 and R_4 in Figure 3) come sufficiently close to one another as to experience an appreciable reduction in their conformational degrees of freedom, with a consequent decrease of the statistical probability. For this reason, unless otherwise stated, we will direct our considerations to the more probable transoid conformation; the cisoid hypothesis will be considered under a separate section, and it will be shown that the overall chain size is only marginally affected by the presence of the cisoid conformations. In either case,

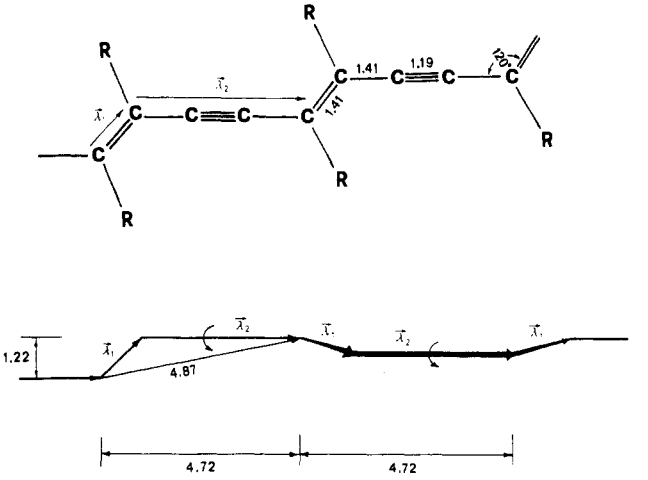

Figure 4. (Above) PDA chain is represented as a sequence of a real C=C bond (λ_1) and of a virtual bond C—C≡C—C (λ_2). (Below) If no twisting or bending fluctuations are permitted, skeletal rotations localized within the virtual bonds cannot decrease the end-to-end chain length below the limit of 4.72 Å per monomeric unit. (Distances in Å.)

the resulting model is a sort of wormlike chain with different bending rigidities in and off its local plane, for which the term "ribbon wormlike chain" may be appropriate. Although at first this appears to be incompatible with the limited conjugation length derived from the optical absorption spectra,[11] it is not unreasonable to expect that future theoretical interpretations may show that some loss of conjugation is entailed by a continuous deformation of the ideal chain geometry. Accordingly, in the following we shall regard the ribbon wormlike chain as a possibly acceptable model (model 1). However, we shall also consider an alternative model (model 2) wherein the loss of conjugation is produced by suitably chosen rotations around chain bonds according to traditional views. More precisely, assuming as a first approximation that the electronic structure is fully described by Figure 1a, internal rotations around either the single or the triple bonds are permitted, to the extent that they consist of cylindrically symmetrical localized bonding orbitals. It is apparent that such rotations would interrupt the electronic conjugation along the chain backbone, since, e.g., they would be incompatible with the resonance structure of Figure 1b. However, it is important to point out that they would not reduce substantially the chain mean-square end-to-end distance. This may be seen from Figure 4, where the crystalline chain conformation is represented as an unsymmetrical zigzag planar sequence of a C=C double bond and of a virtual bond spanning the four atoms (C—C≡C—C); when any flexibility of other chain parameters is neglected, it is easy to check that any set of skeletal rotations exclusively localized on the virtual bonds λ_2 cannot reduce the overall chain length below (4.72N) Å, with an upper limit of (4.87N) Å for full extension, N being the number of monomeric units. (A similar conclusion was reached by Yoon and Brückner after a conformational analysis of n-alkane sequences adjoining rigid blocks in liquid-crystalline block copolymers.)[12]

In conclusion, we shall concentrate on two limiting conformational models:

Model 1. Only twisting and bending fluctuations from the planar, transoid chain structure will be considered, their amplitude being determined from the available vibrational spectroscopy evidence.[13-15]

Model 2. Equiprobable rotations of ±90°, concentrated on the triple bonds with an overall probability $^1/_6$, will also

Table II
Force Constants and Mean-Square Amplitudes of Intramolecular Coordinates q^a

q	$\langle q \rangle$, deg	K_q, mdyn·Å	$\langle \Delta^2 q \rangle = k_B T/K_q$, rad^2
φ (>C=C<)	180	0.51[13] ^{b}	8.11×10^{-3}
φ (C—C)	180	0.51[13] ^{b}	8.11×10^{-3}
θ (C=C—C)	120	0.59[14]	7.02×10^{-3}
θ (C≡C—C)	180	0.26[15]	15.94×10^{-3}

^{a} T = 300 K; φ and θ respectively are rotation and bond angles. See Figure 4 and eq 1. ^{b} Assumed to be equal to the twisting force constant of the double bond of 1,3-butadiene, as determined in ref 13.

be permitted, thus accounting for the average observed conjugation length of 5–7 monomer units.[11]

In-plane bending fluctuations will be allowed to the four skeletal bond angles of each monomer unit, while twisting oscillations will be limited to the single and double bonds (see Figure 1a), and bond-length fluctuations will be disregarded. In view of the small amplitude of all the allowed fluctuations and of the absence of close intramolecular contacts between the chain backbone and the side-group atoms directly bonded to the chain, we shall neglect any correlation either between rotations or between bond angles; in addition, in our calculations we shall neglect long-distance interactions (unperturbed chain). Concerning the average correlation between the rotation angle around any skeletal bond and the valence angles adjacent to it, symmetry reasons make it vanishing. In fact, if $\Delta\varphi$ is the rotational fluctuation from the average planar conformation and $\Delta\theta$ is the bond-angle fluctuation, $\langle \Delta\varphi \Delta\theta \rangle = 0$ because, given $\Delta\theta$, $+\Delta\varphi$ and $-\Delta\varphi$ are equally probable in view of the inherent planar symmetry of the chain. Accordingly, we are left with the problem of evaluating $\langle \Delta^2\varphi_i \rangle$ and $\langle \Delta^2\theta_j \rangle$, which we have solved through the knowledge of the associated force constants and the potential energy equipartition principle within the classical harmonic approximation. We obtain

$$\tfrac{1}{2}k_B T = \tfrac{1}{2}K_q \langle \Delta^2 q \rangle \tag{1}$$

where k_B and T are the Boltzmann constant and the absolute temperature, while K_q and Δq are the force constant and the displacement of the coordinate q from its average, respectively. Table II shows values of K_q, derived from best fitting of infrared data, where q corresponds to the torsion angles φ around the C=C and (C=)C—C(≡C) bonds, both regarded as equivalent to the double bonds of 1,3 butadiene,[13] and also to ∠C=C—C[14] and ∠C≡C—C.[15,16] The associated $\langle \Delta^2 q \rangle$'s at room temperature are also reported. Although to our knowledge no energy parameters for internal rotation around either (≡)C—C or C≡C bonds have been reported in the literature, for the former case we shall approximately adopt the same $\langle \Delta^2\varphi \rangle$ as for the double bonds, while no rotational flexibility around the triple bonds will be assumed apart from the previously discussed rotations of ±90° for model 2. In the absence of these rotations, the four atoms C—C≡C—C are assumed to lie in the conjugation plane, from which the neighboring C=C bonds may slightly depart because of rotational fluctuations around C—C; this simplifying assumption may be justified in terms of conjugation maximization. It should be noted that any inaccuracy concerning the estimated $\langle \Delta^2\varphi \rangle$ for the rotations either around C—C or C≡C reflects very little in the calculated results of the average chain size, both because they are only localized on the long virtual bonds (see Figure 4) and because they may be coupled with the much larger ±90° rotations around the approximately collinear C≡C bonds.

Evaluation of the Mean-Square Chain Size in Solution

We have now enough data to evaluate the average matrices performing the rotation of the Cartesian frame associated with one chain bond to bring it parallel with that associated with the following bond. Let us start from the general expression[17]

$$\mathbf{T}_i = \begin{bmatrix} -\cos\theta_i & -\sin\theta_i & 0 \\ \sin\theta_i \cos\varphi_i & -\cos\theta_i \cos\varphi_i & -\sin\varphi_i \\ \sin\theta_i \sin\varphi_i & -\cos\theta_i \sin\varphi_i & \cos\varphi_i \end{bmatrix} \qquad (i = 1\text{–}4) \tag{2}$$

where the meaning of the rotation and bond angles, φ_i and θ_i, respectively, is shown in Figure 5 ($\varphi_i = 0°$ for a cis conformation). In order to perform the average of $\mathbf{T}_i$, let us first remark that the four average rotation angles $\langle \varphi_i \rangle$ may be all set equal to 180°, while $\langle \theta_3 \rangle = \langle \theta_4 \rangle = 120°$ are the only average bond angles differing from 180°. Using the harmonic approximation, neglecting fourth- and higher-order averages and remembering that $\langle \Delta\varphi_i \Delta\theta_i \rangle = 0$, we have from the above

$$\langle f(q_i) g(q_j) \rangle \simeq \langle f(q_i) \rangle \langle g(q_j) \rangle$$

$$(i \neq j, \text{ f and g stand for cos or sin})$$

$$\langle \cos q \rangle \simeq \cos \langle q \rangle (1 - \tfrac{1}{2}\langle \Delta^2 q \rangle) \tag{3}$$

$$\langle \sin q \rangle \simeq \sin \langle q \rangle (1 - \tfrac{1}{2}\langle \Delta^2 q \rangle)$$

$$(q \text{ stands for either } \varphi_i \text{ or } \theta_i)$$

$$\langle \Delta^2 \varphi_2 \rangle = 0$$

From eq 2 and 3 and Table II we have the following average rotation matrices (see also Figure 5):

$$\langle \mathbf{T}_1 \rangle = \begin{bmatrix} 0.9920 & 0 & 0 \\ 0 & -0.9880 & 0 \\ 0 & 0 & -0.9959 \end{bmatrix}$$

$$\langle \mathbf{T}_2 \rangle_1 = \langle \mathbf{T}_2(\varphi_2 = \pi) \rangle = \begin{bmatrix} 0.9920 & 0 & 0 \\ 0 & -0.9920 & 0 \\ 0 & 0 & -1 \end{bmatrix}$$

$$\langle \mathbf{T}_2 \rangle_2 = \langle \frac{5}{6}\mathbf{T}_2(\varphi_2 = \pi) + \frac{1}{12}\mathbf{T}_2(\varphi_2 = \frac{\pi}{2}) + \frac{1}{12}\mathbf{T}_2(\varphi_2 = -\frac{\pi}{2}) \rangle$$

$$= \begin{bmatrix} 0.9920 & 0 & 0 \\ 0 & -0.8267 & 0 \\ 0 & 0 & -0.8333 \end{bmatrix}$$

$$\langle \mathbf{T}_3 \rangle = \begin{bmatrix} 0.4982 & -0.8630 & 0 \\ -0.8595 & -0.4962 & 0 \\ 0 & 0 & -0.9959 \end{bmatrix} = \langle \mathbf{T}_4 \rangle \tag{4}$$

In the above, $\langle \mathbf{T}_2 \rangle_1$ and $\langle \mathbf{T}_2 \rangle_2$ are the rotation matrices around l_{2k} (see Figure 5) with and without the ±90° rotations, respectively, i.e., respectively suited for models 1 and 2. Accordingly, we shall define as follows the matrices for the overall rotation associated with one monomer unit in the two cases:

$$\tau_1 = \langle \mathbf{T}_1 \rangle \langle \mathbf{T}_2 \rangle_1 \langle \mathbf{T}_3 \rangle \langle \mathbf{T}_4 \rangle \tag{4'}$$

$$\tau_2 = \langle \mathbf{T}_1 \rangle \langle \mathbf{T}_2 \rangle_2 \langle \mathbf{T}_3 \rangle \langle \mathbf{T}_4 \rangle$$

Let us note that the two models imply very small deformations of the chain geometry within any given monomer unit. Accordingly, it will be convenient to adopt

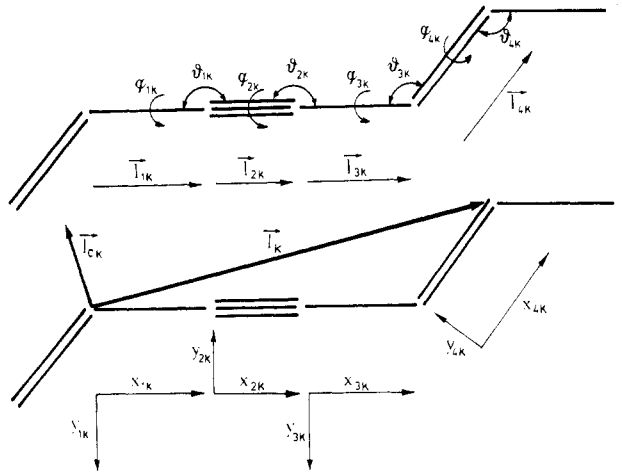

Figure 5. Scheme showing bond vectors, bond and internal rotation angles, virtual bond vectors, and intrinsic Cartesian frames within the kth monomeric unit (z axes are always orthogonal to the paper).

the virtual bond $\mathbf{l}_k$ spanning the kth monomer unit (see Figure 5) to describe the distance between any two units; these virtual bonds will be regarded as rigid, while the atomic mass of the kth monomer unit will be formally concentrated at the common end of $\mathbf{l}_{k-1}$ and $\mathbf{l}_k$. Under these assumptions, according to a well-known statistical result for chains with independent geometrical parameters, we have

$$\langle \mathbf{l}_k \cdot \mathbf{l}_{k+h} \rangle = \text{(in matrix form) } \mathbf{l} \cdot \boldsymbol{\tau}^h \cdot \mathbf{l}^T \tag{5}$$

where

$$\mathbf{l} = [\alpha_x \quad \alpha_y \quad 0]l \tag{6}$$

and $l = 4.87$ Å, $\alpha_x = 0.9681$, $\alpha_y = -0.2507$, and τ is either τ_1 or τ_2 (see eq 4′) according to whether model 1 or model 2 is being considered. In eq 6 $\mathbf{l}$ is represented in the intrinsic Cartesian frame pertaining to the first bond of the general monomer unit (i.e., $\mathbf{l}_{1k}$ in Figure 5). From the above we have[18]

$$C_\infty = \lim_{N\to\infty} \langle r^2 \rangle_{0N}/Nl^2 = [\alpha_x \quad \alpha_y \quad 0](\mathbf{E}+\tau)(\mathbf{E}-\tau)^{-1} \begin{bmatrix} \alpha_x \\ \alpha_y \\ 0 \end{bmatrix} \tag{7}$$

and

$$\langle s^2 \rangle_{0N}/Nl^2 = [\alpha_x \quad \alpha_y \quad 0] \left\{ \frac{N+2}{6(N+1)} (\mathbf{E}+\tau)(\mathbf{E}-\tau)^{-1} - \frac{1}{N+1}\tau(\mathbf{E}-\tau)^{-2} + \frac{2}{(N+1)^2}\tau^2(\mathbf{E}-\tau)^{-3} - \frac{2}{N(N+1)^2}\tau^3(\mathbf{E}-\tau^N)(\mathbf{E}-\tau)^{-4} \right\} \begin{bmatrix} \alpha_x \\ \alpha_y \\ 0 \end{bmatrix} \tag{8}$$

where $\mathbf{E}$ is the unit matrix of order 3, N is the number of monomer units of the chain, τ is either τ_1 or τ_2, $\langle r^2 \rangle_{0N}$ and $\langle s^2 \rangle_{0N}$ respectively are the mean-square end-to-end distance and the mean-square radius of gyration in the unperturbed state, and C_∞ is the unperturbed characteristic ratio defined with respect to the virtual bonds (i.e., $\langle r^2 \rangle_{0N} = C_\infty N l^2$). The connection between C_∞ and the persistence length l_{pers} of the corresponding wormlike chain is easily obtained through the two equivalent expressions of $\langle r^2 \rangle_{0N}$ in the high molecular weight limit (cf. ref 18, Appendix G)

$$\langle r^2 \rangle_{0N} = Nl^2 C_\infty \tag{9}$$

$$\langle r^2 \rangle_{0N} = 2Ll_{pers}$$

where $L = Nl$ is the chain contour length. Equation 9 gives

$$l_{pers} = lC_\infty/2 \tag{10}$$

Temperature Coefficient of the Mean-Square Chain Length

From eq 7, it is not difficult to see that the temperature dependence of C_∞ is mainly embodied in the factor $(\mathbf{E} - \tau)^{-1}$. From eq 3–6 and either model the structure of the matrix τ is of the type

$$\tau = \begin{bmatrix} 1-\epsilon_{11} & \epsilon_{12} & 0 \\ \epsilon_{21} & a-\epsilon_{22} & 0 \\ 0 & 0 & b-\epsilon_{33} \end{bmatrix} \qquad (a, b < 1) \tag{11}$$

where ϵ_{ij} are linear combinations of the mean-square fluctuations $\langle \Delta^2 \varphi_i \rangle$ and $\langle \Delta^2 \theta_j \rangle$ and a and b are temperature-independent constants on the order of unity although smaller than unity. In view of eq 1 we may write

$$\epsilon_{ij} = c_{ij}\, T \ll 1; \qquad (T = 300 \text{ K}) \tag{12}$$

where c_{ij} is temperature independent; the inequality is easily justified considering the figures reported in eq 4. Neglecting ϵ_{ij} in comparison with $(1 - a)$, $(1 - b)$, and products thereof, we get from the above

$$(\mathbf{E}-\tau)^{-1} = \begin{bmatrix} \epsilon_{11}^{-1} & A_{12} & 0 \\ A_{21} & A_{22} & 0 \\ 0 & 0 & A_{33} \end{bmatrix} \tag{13}$$

Here, A_{ij} are constants on the order of unity, therefore much smaller than ϵ_{11}^{-1}. From eq 7 it is now possible to see that C_∞ is given by a sum wherein the dominating term is $\propto \epsilon_{11}^{-1}$, and in view of eq 12 we get

$$C_\infty \simeq \text{constant}/T \tag{14}$$

Accordingly, the current expression of the temperature coefficient of C_∞ gives

$$\mathrm{d} \ln C_\infty/\mathrm{d}t = -1/T \qquad (=-3.33 \times 10^{-3} \text{ at } T = 300 \text{ K}) \tag{15}$$

which agrees within three significant digits with the figure obtained by our numerical results of C_∞ from eq 7 around T = 300 K, for both models 1 and 2.

It may be interesting to point out that eq 14 and 15 are in full agreement with the conclusions derived from the ideal wormlike model, *within the assumption that the squared curvature of the chain is proportional to its local intramolecular energy.*[19,20] (It should be pointed out, though, that in the original definition of the Porod–Kratky model the intramolecular degrees of freedom are assumed to have all the same (zero) internal energy,[21,22] so that C_∞ should be temperature independent.)

In the absence of suitable experimental data, eq 15 must be regarded as a prediction; obviously enough, it is hoped that adequate testing may be provided in the near future.

Results and Comparison with Experiment

Using eq 7 and 10, with the definitions and numerical data given in eq 4, 4′, and 6, we get

model 1: $C_\infty = 78.1$; $l_{pers} = 190.2$ Å

model 2: $C_\infty = 72.8$; $l_{pers} = 177.3$ Å

Both results are in fair agreement with the value (~150 Å) reported in paper 1 from viscosimetric measurements on several polydegraded samples of PTS-12 (see Figure 17 of paper 1 and Table III of this paper). However, we

Table III
Values of Persistence Length Obtained from Fitting Experimental Data Reported in Reference 11[a]

section	polymer	N_w	M_w/M_n	exptl method	l_{pers}, Å
A (polydegraded samples)	PTS-12	several	~2	intrinsic viscosity[b]	150 ± 5
B (polydegraded samples)	PTS-12	several	~2	light scattering[c]	195 ± 5
C (pristine sample)	PTS-12	1253	2.66	light scattering[d]	~165
	PTS-12	1425		light scattering	~165
	PTS-12	2850		light scattering	~200
	P3BCMU	2830		light scattering	~130
	P3BCMU	1020	5.0	light scattering	900 ± 500
	P3BCMU	1700	3.33	light scattering	~290
	P3BCMU	2300	3.94	light scattering	~300
	P3BCMU	1800	3.75	light scattering	~360

[a] Equations 7–10, 16, and 17 of this paper are used. [b] See Figure 17 of ref 11. [c] See Figure 16 of ref 11. [d] See Table VI of ref 11. [e] See Table VII of ref 11.

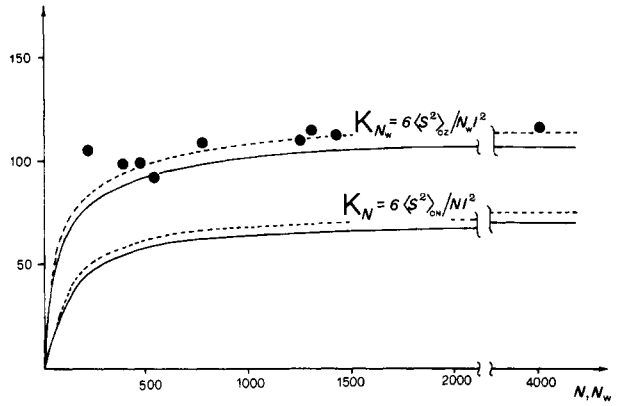

Figure 6. Plots of K_N and K_{N_w} calculated according to eq 8, 16, and 17 for the unperturbed chains (dashed and solid lines for models 1 and 2, respectively). Black dots are the experimental values of K_{N_w} for PTS-12.[11]

believe these measurements give less accurate information than the light-scattering results also reported in paper 1 in view of the several approximations implicit in the solution-viscosity theory. Light-scattering measurements were performed on the above-referred polydegraded samples, the molecular weight distribution of which may be reasonably well described by the Schulz–Flory equation, reading ($M = Nw$, w is the molecular weight of the monomer unit)

$$p(N) = (2/N_w)(1 - 2/N_w)^{N-1}; \qquad \sum_{N=1}^{\infty} p(N) = 1 \qquad (16)$$

which gives $M_w/M_n = 2$. Light-scattering measurement of the mean-square radius of gyration leads to the z-average $\langle s^2 \rangle_z$:

$$\langle s^2 \rangle_z = \sum_N \langle s^2 \rangle_N N^2 p(N) / \sum_N N^2 p(N) \qquad (17)$$

(Note that the zero suffix, standing for "unperturbed value", is reserved to the calculated results.) Figure 6 shows the calculated plots of both $K_N = 6\langle s^2 \rangle_{0N}/Nl^2$ vs. N according to eq 8 ($\lim_{N\to\infty} K_N = C_\infty$) and $K_{N_w} = 6\langle s^2 \rangle_{0z}/N_w l^2$ vs. N_w according to eq 16 and 17 ($\lim_{N_w\to\infty} K_{N_w} = 3/2C_\infty$), together with the experimental points equivalent to K_{N_w} (see Figure 16 of paper 1, where K_{N_w} is denoted C_p). The asymptotic trend of these data gives $C_\infty \simeq 80$, and $l_{pers} \simeq 195$ Å (see also Table III, Section B), with an exceptionally good agreement with model 1 and a reasonably small discrepancy, although beyond experimental error, from model 2 as may be seen in Figure 6. Values of $\langle s^2 \rangle_z$ are also given in paper 1, Table VI, for samples of PTS-12 and P3BCMU, directly obtained from solid-state polymerization. These data are reported in Table III, Section C, together with the best-fitting values of l_{pers}; we believe the poorer consistency among these results may be partly ascribed to departures from the assumed Schulz–Flory distribution. In particular, the systematic increase of l_{pers} over the average, when $M_w/M_n > 2$, may be easily rationalized.

Table IV
Model 1: Comparison of $\langle s^2 \rangle_{0,N}/Nl^2$[a]

N	$\langle s^2 \rangle_{0,N}/Nl^2$ from eq 8	$\langle s^2 \rangle_{0,N}/Nl^2$ from eq 18	% diff
128	6.321	6.278	0.68
256	8.650	8.601	0.57
512	10.492	10.459	0.31
1024	11.649	11.640	0.07
2048	12.310	12.303	0.05

[a] Evaluated through the rotation-matrix algorithm and compared with the figures obtained for the ideal wormlike chain with the same persistence length.

In spite of the better agreement of model 1 with the experimental results, we want to point out that either some amount of excluded-volume effects or some inaccuracy in the force constants adopted by us (see following) could deceive a higher chain stiffness from the light-scattering data. Therefore it appears premature to favor one or the other model on the basis of these comparisons alone.

A comment concerning the electronic structure reported in Figure 1b may be of some interest. If we assume that it represents the actual chain structure, it would seem appropriate to consider the single bond as having the same twisting force constant as found for the central bond of 1,3-butadiene, i.e., $K_\varphi = 0.109$ mdyn·Å from ref 13 (see Table II for the other force constants). With no change in the other parameters, this would produce $C_\infty = 52.0$ and $l_{pers} = 127$ Å (from eq 7 and 10, respectively), with a very substantial disagreement from experiment. This result may be regarded as still another evidence that the structure of Figure 1b is a minor component.

Adequacy of the Wormlike Model

It should be stressed that in spite of the adoption of a matrix treatment that is currently applied to flexible polymer chain with independent skeletal rotations, our results are in excellent agreement with those expected for an ideal wormlike chain with the appropriate value of l_{pers}. This is shown in Table IV where the values of $\langle s^2 \rangle_{0N}/Nl^2$ from eq 8, model 1, are reported for some typical lower values of N, together with those evaluated for the ideal wormlike chain according to the equation

$$\langle s^2 \rangle_{0N} = \frac{2L^2}{y^4}\left(-1 + y - \frac{1}{2}y^2 + \frac{1}{6}y^3 + e^{-y}\right) \qquad (18)$$

($y = L/l_{pers}$, $L = Nl$, $l_{pers} = 190.22$ Å, $l = 4.87$ Å)

The average disagreement is about 0.3% and is obviously tending to 0 for large N. Accordingly, it must be concluded

Table V
Cross-Vectors Characteristic Ratio of PDA Chains ($C_{C,\infty}$) and Comparison with C_∞[a]

	$C_{C,\infty}$	C_∞	$l_{pers} = lC_\infty/2$
model 1[b]	60.9	78.1	190.2 Å
model 2[c]	13.3	72.8	177.3 Å
fictitious model[d]	6.6	72.1	175.6 Å

[a] See text. [b] Ribbon wormlike model; see Figure 2. [c] Same as model 1, with $^1/_6$ overall probability for ±90° rotations. [d] Overall probability of $^2/_3$ for ±90° rotations.

that in spite of its ribbonlike structure, the chain is quite adequately described by the wormlike model. If the same comparison is applied to model 2, the disagreement increases to an average of 0.6% and shows an opposite sign. In other words, models 1 and 2 respectively appear to be (slightly) more and less flexible than a wormlike chain with the corresponding value of l_{pers}. (Note that "flexibility" here stands for rapid loss of correlation between vectors $\mathbf{l}_k$ of consecutive monomer units, see Figure 5.)

Longitudinal and Lateral Chain Flexibility

Given the local ribbon wormlike structure of the chain, it appeared of some interest to compare the overall degree of correlation among vectors tangential to the chain axis ($\mathbf{l}_k$ in Figure 5), as embodied in the characteristic ratio C_∞, with that among vectors $\mathbf{l}_{Ck}$ at right angles with $\mathbf{l}_k$, contained in the plane defined by the four skeletal bonds of the general monomer unit. Referring to Figure 5, the components of the general unitary cross vector $\mathbf{l}_{Ck}$ in the framework of skeletal bond $\mathbf{l}_{1k}$ are (see eq 6)

$$\mathbf{l}_C = [-\alpha_y \quad \alpha_x \quad 0] \tag{19}$$

The characteristic ratio $C_{C,\infty}$ of these cross vectors is given exactly as in eq 7 except for the substitution of $\mathbf{l}_C$ for the vector $[\alpha_x \quad \alpha_y \quad 0]$ (and its transpose). As expected, $C_{C,\infty}$ is strongly influenced by the existence of rotations around the triple (or the single) chain bonds, unlike C_∞; this is shown in Table V where a fictitious model with equiprobable rotations of 0°, +90°, and −90° around the triple bond is also considered together with models 1 and 2. In principle, $C_{C,\infty}$ might be revealed by measuring the mean-square dipole moment in solution of suitable PDA chains with one dipolar substituent per monomer unit.

Allowing for the Cisoid Conformation

As previously discussed, such a conformation appears to be statistically unfavored with respect to the transoid one; in fact, the distance between the two C atoms directly bonded to the main chain within the side groups R_1 and R_4 (see Figure 3) is ~3.9 Å, which must inevitably entail some decrease in steric freedom of the groups themselves. Nevertheless, we have also evaluated C_∞ and $C_{C,\infty}$ for two models containing cisoid conformations. Specifically, in addition to all the parameters of the previous models, we have assumed either (i) equal probabilities for the transoid and the cisoid conformation or (ii) same as in (i) plus ±90° rotations with $^1/_6$ overall probability. We soon realized that both models lead to the same result; in fact, they have the same matrix $\langle \mathbf{T}_2 \rangle$ consisting of the same (1,1) element as in eq 4, all other elements being 0. The results are $C_\infty = 72.0$, $C_{C,\infty} = 5.7$ (compare with Table V), and we have verified that the corresponding curves calculated for K_N and K_{N_w} are virtually indistinguishable from those related to model 2 (solid lines in Figure 6).

Concluding Remarks

Through the use of the classical rotation-matrix algorithm we have shown that the dimensions of PDA chains in solution may be described surprisingly well by a model consisting of a single rotational isomer, which may only undergo twisting and bending oscillations around the conformational energy minimum (model 1). Alternatively, a limited amount of ±90° rotations around the triple bonds may be assumed (model 2), with a limited reduction of the mean-square chain size (<7%). However, both models are based on a few approximations, among which is the neglect of excluded-volume effects, that might cast some doubts on the significance of the present calculations as related to the experimental data. Unfortunately, the pronounced polydispersity of the samples and the insufficient accuracy of our data do not allow a Sharp–Bloomfield[23] analysis of the radius of gyration, which could help, e.g., to estimate the influence of the excluded volume, yielding a more realistic "unperturbed chain stiffness". This fact prevents our favoring any of the conjugation models under consideration by means of the molecular dimensions, the more so because of their relatively small difference (see also Figure 6; note that results for the less probable models where a cisoid conformation is allowed are virtually indistinguishable from model 2). However, it should be pointed out that model 2 appears to give a more satisfactory interpretation of the effective conjugation length according to the current views, while the slight deviation from the experimental chain size may be attributed either to a small excluded-volume expansion or, perhaps more likely, to some uncertainty about the value of the torsional force constant K_φ for the double bond, which plays a very critical role in determining the molecular dimensions (see above). Model 2 is therefore the one that describes both the molecular dimensions and the spectroscopic data to a satisfactory degree. Incidentally, the cross-vector characteristic ratio (see Table V) yields a cross-vector persistence length $l_{C,pers} = C_{C,\infty}l/2$, whence a cross-vector correlation degree $C_{C,\infty}/2$ (in monomer units) may be obtained. While this parameter is 6.65 for model 2, i.e., corresponding to the assumed conjugation length, for model 1 we have 30.45, which might be roughly taken as an "effective" conjugation length for the ideal ribbon wormlike model.

As a final remark, we recall that any "softening" of the twisting force constant around the double bond of the electronic structure reported in Figure 1a, as required if the cumulene structure of Figure 1b is to have any significant weight, leads to a dramatic decrease of l_{pers} (>30% if the pure cumulene structure is considered). For the same reasons, a cis conformation of the double bonds, as sometimes discussed in the literature, can be considered only in a very small amount (i.e., less than one in a persistence length, or ≈ 2.5%).

Acknowledgment. This study was performed with financial support from the "Piano Finalizzato per la Chimica Fine e Secondaria", CNR, Italy.

Registry No. PTS-12 (homopolymer), 81723-80-0; P3BCMU (homopolymer), 68777-87-7; PTS-12 (SRU), 91490-81-2; P3BCMU (SRU), 70221-28-2.

References and Notes

(1) Wegner, G. *Z. Naturforsch., B: Anorg. Chem. Org. Chem.* **1969**, *24B*, 824.
(2) Wegner, G. *Makromol. Chem.* **1971**, *145*, 85.
(3) Wegner, G. In "Molecular Metals"; Hatfield, W. E., Ed.; Plenum Press: New York, 1979; p 209 ff.
(4) Baughman, R. H. *J. Appl. Phys.* **1972**, *43*, 4362.
(5) Baughman, R. H. *J. Polym. Sci., Polym. Phys. Ed.* **1974**, *12*, 1511.
(6) Bloor, D. In "Developments in Crystalline Polymers"; Basset, D. C., Ed.; Applied Science: London, 1982; p 155 ff.
(7) Bloor, D.; Preston, F. H.; Ando, D. J.; Batchelder, D. N. In "Structural Studies of Macromolecules by Spectroscopic

Methods"; Ivin, K. J., Ed.; Wiley: New York, 1976; p 91 ff.
(8) Siegel, D.; Sixl, H.; Enkelmann, V.; Wenz, G. *Chem. Phys.* **1982**, *72*, 201.
(9) Enkelmann, V. *Adv. Polym. Sci.* **1984**, *63*, 91.
(10) Baughman, R. H.; Chance, R. R. *J. Polym. Sci., Polym. Phys. Ed.* **1976**, *98*, 481.
(11) Wenz, G.; Müller, M. A.; Schmidt, M.; Wegner, G. *Macromolecules* **1984**, *17*, 837. (Also referred to as paper 1.)
(12) Yoon, D. Y.; Brückner, S. *Macromolecules* **1985**, *18*, 651.
(13) Furukawa, Y.; Tacheuchi, H.; Harada, I.; Tasumi, M. *Bull. Chem. Soc. Jpn.* **1983**, *56*, 392.
(14) Zannoni, G.; Zerbi, G. *J. Mol. Struct.* **1983**, *100*, 485.
(15) Zerbi, G.; Gussoni, M. *J. Chem. Phys.* **1964**, *41*, 456.
(16) It must be pointed out that rigorously speaking eq 1 applies to the general normal mode; however, in the present case the approximation is very good considering that the ratios between the cross and the diagonal force constants are very small[13-15] and that the relative differences between the eigenvalues and the K_q's are quadratic functions of those ratios.
(17) Allegra, G.; Flisi, U.; Crespi, G. *Makromol. Chem.* **1964**, *75*, 189.
(18) Flory, P. J. In "Statistical Mechanics of Chain Molecules"; Interscience: New York, 1969; Chapter 1 and Appendix G.
(19) Saitô, N.; Takahashi, K.; Yunoki, Y. *J. Phys. Soc. Jpn.* **1967**, *22*, 219.
(20) Ronca, G.; Yoon, D. Y. *J. Chem. Phys.* **1982**, *76*, 3295.
(21) Porod, G. *Monatsh. Chem.* **1949**, *80*, 251.
(22) Kratky, O.; Porod, G. *Recl. Trav. Chim. Pays-Bas* **1949**, *68*, 1106.
(23) Sharp, P.; Bloomfield, V. A. *Biopolymers* **1968**, *6*, 1201.

Conformational Statistics of Poly(methyl methacrylate)

M. Vacatello*† and P. J. Flory

IBM Research Laboratory, San Jose, California 95193. *Received March 25, 1985*

ABSTRACT: Conformational energy calculations have been carried out for monomeric and trimeric oligomers of PMMA and for four-bond segments (embracing two repeat units) embedded in stereoregular PMMA chains, including both isotactic (meso) and syndiotactic (racemic) stereoisomeric forms. All incident interactions were taken into account. In each conformational domain the energy was minimized with respect to all bond angles and torsion angles including the torsional rotation χ of the ester group about the bond joining it to the chain backbone. Although in most of the conformations the plane of the ester group tends to occur approximately perpendicular to the plane defined by the adjoining skeletal bonds, substantial departures occur when one of these bonds is in a gauche $\bar{g}$ state. In consequence of this departure from $\chi = 0$ or π, the energy of the $\bar{g}$ conformations is not excessive, as was originally concluded. The intradiad bond angle $\tau' = 124 \pm 1°$ in all conformations after energy minimization. The interdiad bond angle $\tau = 106°$ when both adjoining skeletal bonds are trans t, $\tau \approx 111°$ when one bond is t and the other g or $\bar{g}$, and $\tau \approx 116°$ when both are g or $\bar{g}$. The spatial configurations found to be of lowest energy for stereoregular chains are in excellent agreement with crystallographic studies on i-PMMA and with results of wide-angle X-ray scattering of s-PMMA. The backbone torsional angles for the various energy minima can be represented approximately by six discrete states that form the basis for a rotational isomeric state treatment. Conformations near trans are preferred; the preference is pronounced for s-PMMA. Characteristic ratios and their temperature coefficients calculated according to the six-state scheme are in satisfactory agreement with experimental results. Parameters used in these calculations follow directly from the conformational energy calculations; adjustments are not required.

Introduction

The conformations accessible to poly(methyl methacrylate) (PMMA) chains were investigated by Sundararajan and Flory[1] on the basis of a simple rotational isomeric state (RIS) scheme with each skeletal bond assigned to either the trans t or the gauche g conformation. The alternative gauche $\bar{g}$ state was dismissed on the grounds that steric repulsions between atoms of the ester group and groups attached to the neighboring substituted skeletal carbon C^α (see Figure 1) were found to be acute in this conformation. Additionally, the skeletal bond angle τ_k, defined in Figure 1, was assumed to be 110° irrespective of the conformations of the adjoining skeletal bonds.

The steric repulsions operative in the $\bar{g}$ conformation depend on the orientation of the ester group[2] specified by the angle χ_k that measures the torsion about the C^α–C* bond; see Figure 1. Orientations $\chi = 0$ or π, in which the plane of the ester group is perpendicular to the plane defined by the adjoining skeletal bonds, were originally considered[1] to dominate all other possibilities owing to influences of steric interactions involving the skeletal methylene groups. This premise appeared to be supported by infrared absorption spectra of syndiotactic PMMA[3] and of model compounds[4] in the 1050–1300-cm^{-1} region. On the other hand, dielectric and mechanical relaxation measurements[5] indicate a greater diversity of orientations for the side groups. Conformational energy calculations subsequently carried out by Sundararajan[2] show that relaxation of the restriction of χ to values of 0 and π may facilitate occurrence of the $\bar{g}$ state in the vicinity of $\phi = -100°$ to $-120°$ (see ref 6 on conventions pertaining to the signs of torsional angles ϕ). Furthermore, recent FTIR investigations[8,9] on hydrogeneous and deuterated PMMA samples cannot be reconciled with the two-state scheme used previously; additional gauche states for the skeletal bonds are required to account for these results.[8,9]

Recent calculations on polyisobutylene[10] demonstrate that reliable conformational analysis of disubstituted vinyl polymers requires explicit allowance for the variability of the bond angles with conformation and for orientation correlations between substituents separated by several bonds. We present in this paper the results of a conformational analysis of PMMA in which all the bond angles and torsion angles have been treated as free variables subject to optimization. Using the outcome of preliminary calculations on simple models as starting point, we have minimized the energies of all eligible regular conformations for both isotactic and syndiotactic PMMA. The results are discussed in terms of a six-state RIS scheme.

Energy Calculations

Intramolecular conformational energies were calculated as sums of contributions from bond angle deformations, inherent torsional potentials, nonbonded interactions be-

†Permanent address: Dipartimento di Chimica, Università di Napoli, Via Mezzocannone 4, 80134 Naples, Italy.

0024-9297/86/2219-0405$01.50/0